Aggregation of Methylene Blue in Frozen Aqueous Solutions Studied by Absorption Spectroscopy

Dominik Heger,[†] Jaromír Jirkovský,[‡] and Petr Klán*,[†]

Department of Organic Chemistry, Faculty of Science, Masaryk University, Kotlarska 2, CZ-611 37 Brno, Czech Republic, and J. Heyrovsky Institute of Physical Chemistry, Academy of Sciences of the Czech Republic, Dolejskova 3, CZ-18223 Praha, Czech Republic

Received: January 25, 2005; In Final Form: June 7, 2005

The paper presents a qualitative as well as quantitative spectroscopic study of methylene blue (MB) aggregation that occurs upon freezing the aqueous solutions over a wide concentration range. The Gaussian curve analysis and the multivariate curve resolution−alternating least squares method were used to determine the number and concentration of chemical species responsible for the overlaying absorption visible spectra measured. The results show the extent of aggregation for the concentrations above 10^{-7} mol L^{-1}, being dependent on the freezing rate and the initial concentration. While the local concentration of MB at the grain boundaries of polycrystalline ice increased by approximately 3 orders of magnitude upon fast freezing at 77 K compared to the liquid phase, the concentration raised at least by 6 orders of magnitude upon slow freezing at 243 K. Since enhancement of the local concentration of solutes plays an important role in (photo)chemical transformations in solid aqueous media, this work helps to understand how the initial conditions control the course of the process. The results are relevant in other interdisciplinary fields, such as environmental chemistry, cosmochemistry, or geochemistry.

1. Introduction

Upon freezing aqueous solutions of organic compounds, most chemical and physical processes are slowed since the phase transition radically modifies the reaction microenvironment. The solute molecules accumulate in the unfrozen layer surrounding the crystal walls, at the grain boundaries, and are not incorporated much into the solid polycrystalline ice.[1−5] Furthermore, fast nonequilibrium freezing can generate a substantial electrical potential difference between the solid ice and an unfrozen liquid layer.[6,7] As temperature further decreases, the solute concentration becomes high[7−9] and the layer eventually solidifies. Aggregated organic molecules in such a heterogeneous mixture undergo remarkable photochemistry[9−11] that can have large environmental consequences in polar regions,[12−16] where chromophoric organic pollutants are common trace constituents of natural ice and snow.[17−19]

Methylene blue (MB) is a cationic dye which exhibits two major absorption bands at 293 ($\pi-\pi^*$) and 664 ($n-\pi^*$) nm in dilute aqueous solutions,[20] the latter having a shoulder at 610 nm corresponding to the 0−1 vibronic transition.[21−23] It is well-known that the aggregation of MB has a significant effect on its optical properties. The face-to-face (sandwich-type, H-aggregates) associations of this cationic dye (Scheme 1) show the blue shift of the spectral band of the $\pi-\pi^*$ transition, while the head-to-tail (J-type) arrangement shows the red shift.[24] The H-type aggregates are typically observed in aqueous solutions. While the ∼664-nm band is assigned to an isolated molecule (monomer), a shift to 605 nm, accompanied by a second maximum at 697 nm, is observed when dimer forms, and an additional blue shift to 575 nm appears when trimer forms,[22,25] being supported by the exciton splitting theory.[24] The reported equilibrium constants for the dimerization[22,26,27] and trimerization[25] steps, $2-10 \times 10^3$ L mol^{-1} and 6×10^6 L^2 mol^{-2}, respectively, suggest that the latter process is largely preferred at higher concentrations. In addition, Zhao and Malinowski determined the dissociation constant of trimer (3.2×10^{-11} L^3 mol^{-3}) by a window factor analysis, suggesting that one chlorine anion is incorporated into the trimer structure.[28] The molar absorption coefficients for monomer, dimer, and trimer were reported within $4-9 \times 10^4$ M^{-1} cm^{-1}.[25] The spectral characteristics of higher aggregates are distinct from each other indicating the strong π-interactions among MB molecules; the self-organization is promoted by electrostatic and dispersion forces as well as by hydrophobic effects.[29] The association effect is strongly affected by dye surroundings, causing that higher MB concentrations are required to obtain the same level of aggregation in organic solvents compared to water. The dye has been frequently used to study molecular aggregations on solid surfaces.[30] In this work, we benefited from this technique to probe the aggregation of MB in frozen aqueous solutions as an archetype for such a behavior of other organic molecules.

2. Experimental Section

Methylene blue (purum, Fluka) was used without further purification and each experiment was performed with a freshly prepared stock solution. Water was purified by the reverse osmosis process on an Aqua Osmotic 03 and its quality complied with U.S. Pharmacopeial Standards (USP). The solidified samples in Plastibrand cuvettes (transparent at >280 nm) containing MB solutions were prepared by freezing either quickly at 77 K (a liquid nitrogen bath) or slowly at 243 K (freezer). The spectra of liquid aqueous solutions were measured on a Unicam UV4 (Cambridge, U.K.) against a pure water

* Author to whom correspondence should be addressed. Phone: +420-549494856; fax: +420-549492688; e-mail: klan@sci.muni.cz.
[†] Masaryk University.
[‡] J. Heyrovsky Institute of Physical Chemistry.

10.1021/jp050439j CCC: $30.25
Published on Web 07/12/2005

SCHEME 1

sample in quartz cells with optical path lengths varied from 0.01 to 5 cm. The spectra of frozen samples and the reference spectra of pure ice were measured on a Lambda 19 UV/VIS/NIR spectrophotometer (Perkin-Elmer) using a 60-mm integrating sphere (the slit width was set to 1 nm and the scan speed to 480 nm min^{-1} or lower) immediately after removing the cuvettes from the cold environment. Although the sample temperature was not controlled during the absorption measurements, no changes of the spectra were observed within the time period necessary for duplicate consecutive experiments. The averaged spectral background of pure ice was subtracted from each spectrum, and the spectra shown are averaged from at least three independent measurements. Heterogeneity and lower transparency of the polycrystalline ice samples decreased the signal-to-noise ratio, and a band broadening can be attributed to light scattering and reflection. The final spectra were smoothed using an adjacent averaging method when necessary.

Origin 7.0 and MATLAB 6.5.1 were utilized as the graphical and statistical software. The multivariate curve resolution−alternating least squares (MCR-ALS) method has been used as a model-free mathematical method for recovery of the concentration profiles and pure spectra of the spectroscopically active species, on the basis of the Lambert−Beer law and a least squares minimization.[31] The first step in the recovery was finding the number of species in the sample by a singular value decomposition (SVD) of the data in MATLAB. The evolving factor analysis (EFA) routine was applied for estimation of the concentration profiles and was subsequently used for MCR-ALS with specific constrains applicable in this calculation (e.g., non-negativity, unimodality, or closure), developed by Tauler and his collaborators.[32,33] The step by step filter program[34,35] was applied to determine the number of peaks in the spectra.

3. Results

3.1. Liquid MB Solutions (293 K). Monomers and oligomers of MB in liquid aqueous solutions can be easily distinguished by absorption spectroscopy; analyses of the overlaying spectra have been reported in several studies.[22,29] This paragraph serves for setting and adjusting the technique applied later on the frozen solutions of MB as well as for comparing different approaches to the problem, including calculations based on the reevaluated equilibrium constants.

Gaussian Curve Fitting. Visible absorption spectra of the samples at 293 K (Figure 1a) were measured and fitted with the Gaussian curves (the *GaussAmp* function against cm^{-1} in the Origin software). The analysis, described in the Supporting Information in detail, revealed three species with maxima matching the known literature values: monomer with the maxima at 15 060 and 16 026 cm^{-1} (664 and 624 nm, respectively) clearly observable for concentrations in the interval of $\sim 5 \times 10^{-7}$ and $\sim 10^{-5}$ mol L^{-1} and dimer and trimer with the maxima at 16 502 and 17 699 cm^{-1} (606 nm and 565 nm, respectively) for concentrations above $\sim 10^{-5}$ mol L^{-1}. Two additional peaks in the interval of 17857−16750 cm^{-1} (560−597 nm) appeared above 10^{-4} mol L^{-1} and were employed in the calculations. They supposedly correspond to the overlaying spectra of trimer and higher oligomers. Increase in the dimer concentration at the expense of that of monomer, and a successive appearance of higher aggregates, is advocated by a shift of the maximum rather than a band broadening (the insert in Figure 1a).

The abundances (standardized concentrations) of the species, shown in Figure 1b, were calculated from the integrated peak areas and were corrected on the molar absorption coefficients obtained by the MCR-ALS method. A standardized concentration represents the fraction of the concentration of a given species over a sum of all concentrations for each MB species, and it is expressed in the terms of the monomer concentration. The relative abundances of trimer and higher aggregates were merged into one curve. Figure 1b provides the qualitative interpretation of the abundances; the aggregation process, a formation of dimer and trimer, was preferred at the initial MB concentration above 10^{-3} mol L^{-1}, where the total fraction of monomer is below 0.5 (50%).

To compare the abundance profiles, the equilibrium constants of dimerization and trimerization have been estimated to support our experimental data. While Braswell[25] calculated the constants from the assumption that trimer is formed directly from monomer, an assumption that trimers are formed from dimers has been added to our calculations. The Gaussian fitting analysis following by MCR-ALS calculations provided the concentrations of the MB species and the molar absorption coefficients. The resulting equilibrium constants, 282 ± 14 and $(9.1 \pm 4.2) \times 10^3$ L mol^{-1} for dimerization and trimerization, respectively, were evaluated by the method of a straight line fitting (see Supporting Information). The confidence intervals were received for a 90% probability.

Multivariate Curve Resolution. The latest release of MCR-ALS Graphical User-Friendly Interface was used to resolve the spectra and concentration profiles by a mathematical least-squares minimalization.[32] The absorbances were calculated for a 1-cm optical path length and the closure was set to the real concentrations. In case of other constrains, the fast nonnegative least squares and unimodality (with an average implementation and the constraint tolerance equal to 1.05) were applied for all concentrations and spectra.

A MCR-ALS method was applied for the same initial data as those in the Gaussian curve analysis. SVD revealed three significant species present in the mixture. In the first case, the spectra and concentration profiles for "pure" species were obtained from the MCR-ALS method using input data calculated by the evolving factor analysis (EFA) (Figure 2a and 2b). The spectrum of monomer (Figure 2a; black line) is composed of two overlying peaks, from which one apparently belongs to the known monomer absorption band (15040 cm^{-1}; 665 nm), while that of 16328 cm^{-1} (612 nm) is associated with the 0−1 vibration and the dimer absorption band. The spectrum of dimer (blue line) consists only of one maximum. The dimer concentration in the concentration profile (Figure 2b) is very low compared to the Gaussian analysis (Figure 1b) because of a large molar absorption coefficient of dimer calculated by this method (see Supporting Information).

The resolved spectra and concentration profiles obtained from the MCR-ALS method using input data from the Gaussian fitting analysis showed more realistic results (Figure 3a and 3b) and logically resemble those in Figure 1b as well as data obtained

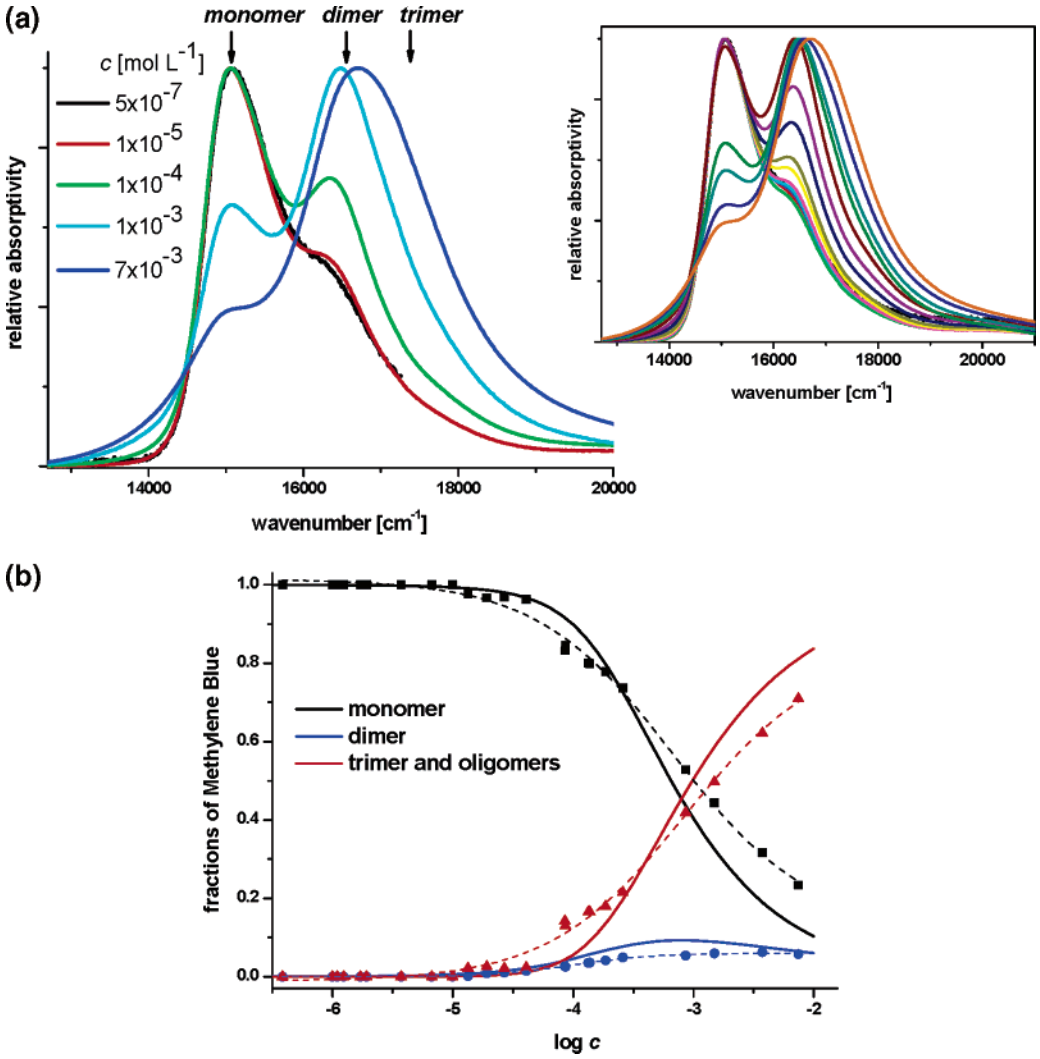

Figure 1. (a) Normalized representative spectra of MB in liquid aqueous solutions at 293 K. The arrows show the known wavenumber values[22,25] corresponding to the absorption maxima of individual species. The insert displays the spectra of all samples at concentrations in the interval of 5.0×10^{-7}–7.5×10^{-2} mol L^{-1}. (b) The concentration-dependent abundances obtained by the Gaussian fitting analysis (solid points; monomer, black; dimer, blue; trimer and oligomers, red; the dotted lines are nonlinear regression fits) in samples at 293 K as a function of the MB concentration *c*. The solid lines represent the calculated concentration profiles obtained from the estimated equilibrium constants.

from the estimated equilibrium constants. The spectrum of monomer exhibits a maximum at 15 050 cm^{-1} (664 nm) and a shoulder maximum at 16 130 cm^{-1} (620 nm); that of dimer has a maximum at 16 480 cm^{-1} (607 nm) with a second minor band at 14 600 cm^{-1} (685 nm). Such findings correspond well to the observation of Bergmann and O'Konski.[22] The spectrum of trimer is broader and consists of three peaks: 17 319 cm^{-1} (577 nm), 15 877 cm^{-1} (630 nm), and 14 558 cm^{-1} (687 nm). Both minor maxima are artifacts of the absorption bands corresponding to those of monomer and dimer. A comparison of all calculated profiles is shown in Figure 4, providing a good agreement of the calculation methods applied, according to which an efficient dimer and trimer formation occurs at the initial MB concentrations above $\sim 10^{-3}$ mol L^{-1}.

3.2. Solid MB Solutions (77 K). The data obtained from the spectral analysis of differently frozen MB aqueous solutions were used to identify the aggregation species present in this constrained medium and to make qualitative estimation of their concentrations.

Gaussian Curve Fitting. A relatively fast freezing rate of the aqueous MB samples immersed in a liquid nitrogen bath (77 K) caused a significant change of the relative abundances of the MB species and new significant blue-shifted absorption bands (Figure 5a) compared to liquid solutions. The lowest initial concentration, for which the signal had reproducible character, was 2.25×10^{-7} mol L^{-1} because of a lower signal-to-noise ratio. In this case, two Gaussian curves were readily fitted having the maxima at 15 383 cm^{-1} (650 nm) and 16 908 cm^{-1} (591 nm), and they were assigned to the monomer and trimer absorption bands, shifted by ~10 nm compared to liquid samples. The highest concentration, where traces of monomer were still resolved, was found as low as 2.25×10^{-6} mol L^{-1}. Samples with higher concentrations exhibited absorption in the interval between 15 823 cm^{-1} (632 nm) and 16 450 cm^{-1} (608 nm), and it was assigned to dimer. The concentration profile obtained by this analysis is shown in Figure 5b, where the monomer and dimer concentrations are summed up. Trimer prevailed already at the lowest MB concentrations, and the largest peak in the spectrum had the maximum between 18 416 and 19 305 cm^{-1} (543 and 518 nm), which is considered to correspond to higher aggregates of MB, dominating at concentrations above $\sim 5 \times 10^{-6}$ mol L^{-1}.

Multivariate Curve Resolution. A similar MCR-ALS analysis as described in paragraph 3.1 was applied to absorption data of the frozen MB solutions at 77 K (in contrast, the spectra were normalized to the maximum height of peaks prior to the analysis

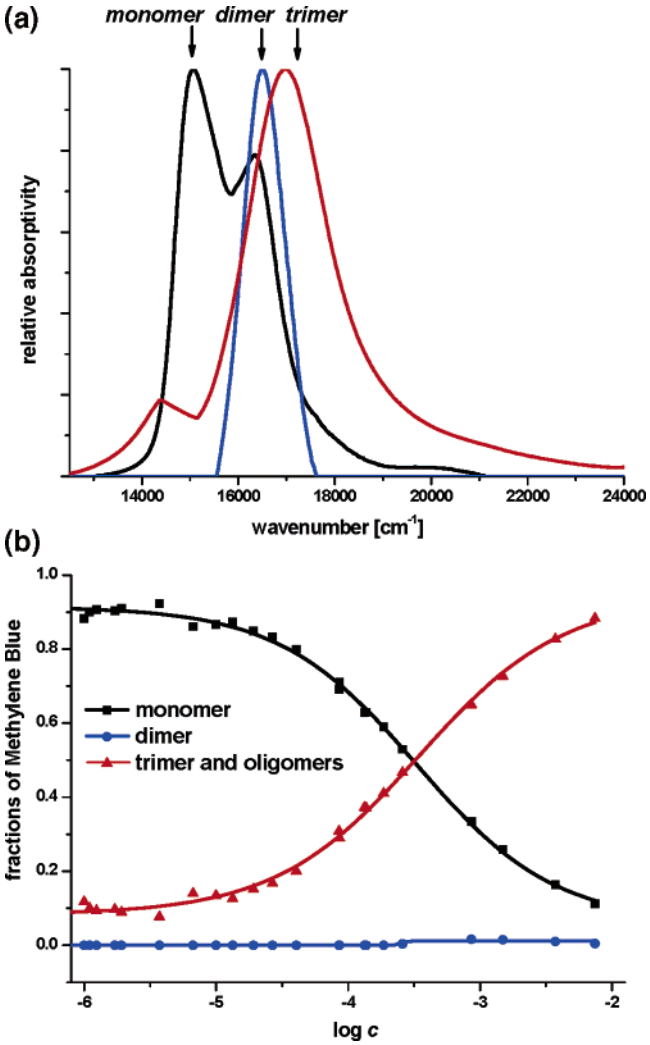

Figure 2. (a) Calculated normalized spectra of three MB species (black, monomer; blue, dimer; red, trimer) in liquid aqueous solutions at 293 K obtained from MCR-ALS method using input data calculated by the evolving factor analysis (EFA). The arrows show the known wavenumber values[22,25] corresponding to the absorption maxima of individual species. (b) The calculated relative concentration-dependent abundance profiles in samples at 293 K as a function of the MB concentration *c* obtained from the MCR-ALS method on the basis of data from Figure 2a. The lines are visualized trends of the corresponding calculated values (solid points).

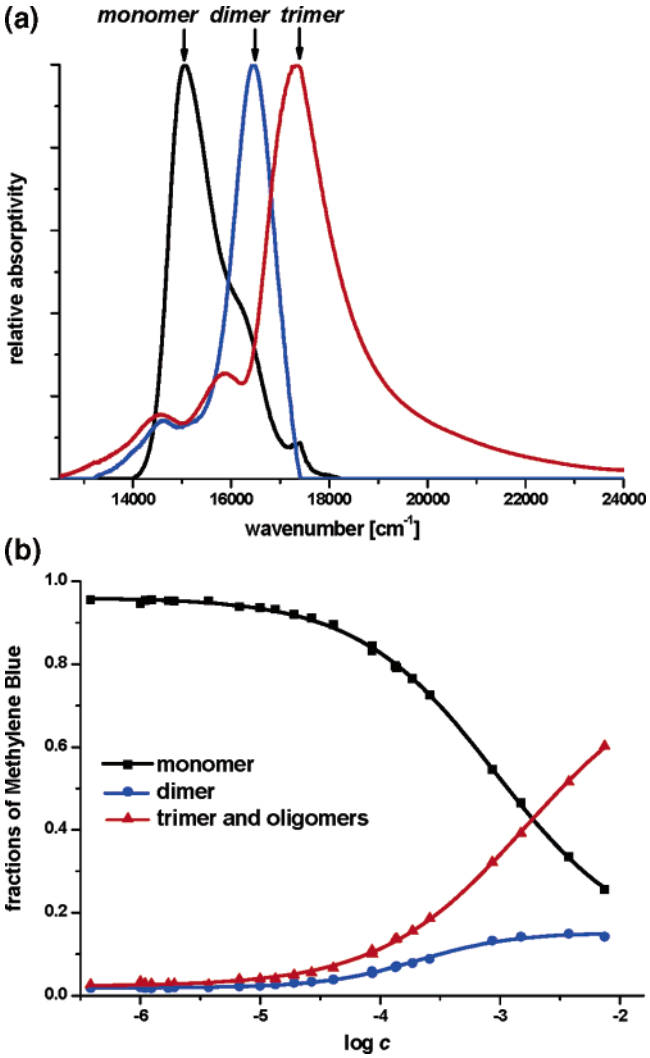

Figure 3. (a) Calculated normalized spectra of three MB species (black, monomer; blue, dimer; red, trimer) in liquid aqueous solutions at 293 K obtained from the MCR-ALS method using input data from the Gaussian fitting analysis. The arrows show the known wavenumber values[22,25] corresponding to the absorption maxima of individual species. (b) The calculated relative concentration-dependent abundance profiles in samples at 293 K as a function of the MB concentration *c* obtained from the MCR-ALS method on the basis of data from Figure 3a. The lines are visualized trends of the corresponding calculated values (solid points).

and the closure constant was set to 1). The sample with the lowest concentration (2.25×10^{-7} mol L^{-1}) was not available because of an insufficient quality of the signal. Figure 6a and 6b shows data calculated by the evolving factor analysis while Figure 7a and 7b presents those received from the Gaussian fitting analysis. The spectra of the "pure" MB species were not resolved in this case; instead, the absorption curves represent three mathematically resolved species that generally correspond to the individual aggregates or to their mixtures (Figures 6a and 7a). Since the abundance of monomer and dimer was very low even at the lowest concentrations, the concentration profiles are simple and comparable in both cases. It is clearly established again that higher aggregates dominate in samples with concentrations above $\sim 5 \times 10^{-6}$ mol L^{-1}.

3.3. Solid MB Solutions (243 K). The absorption signal of MB samples frozen slowly in the refrigerator at 243 K was quite weak and noisy (the samples were visually heterogeneous), however, precipitation of MB was never observed visually unless samples were frozen very slowly above 260 K. Slow freezing affected the relative abundances of the MB species noticeably more than fast freezing, and there are only two significant broad blue-shifted absorption bands as portrayed in Figure 8. The spectra obtained from the Gaussian fitting analysis barely revealed the existence of dimer and trimer in samples with the lowest concentrations, however, the maxima at 19 608−19 881 cm^{-1} (510−503 nm) and 20 833−21 368 cm^{-1} (480−468 nm) belong definitively to the most abundant species that must correspond to high-weight aggregates not observed in liquid or even in quickly frozen aqueous samples. The attempts to apply MCR-ALS model analysis were not successful in this case since the spectra were comparable in the whole concentration range. For comparison, the samples containing MB in KBr tablets, measured at the mass ratios (MB/KBr) 5×10^{-4} and 5×10^{-5}, provided spectra, the main peak of which was found at 18 520 cm^{-1} (540 nm) and shoulders at 15 015 and 16 390 cm^{-1} (666 and 610 nm, respectively); thus, higher aggregates were present together with monomer and lower aggregates, in contrast to frozen solutions at 243 K.

TABLE 1: Changes in the Concentrations of the MB Species[a]

sample	calculation method[b]	M/(D + T) (mol L^{-1})	(M + D)/T (mol L^{-1})	(M + D + T)/higher oligomers (mol L^{-1})
liquid (293 K)	GFA	6×10^{-4}	1×10^{-3}	
	MCR-ALS/EFA	3×10^{-4}	3×10^{-3}	
	MCR-ALS/GFA	1×10^{-3}	2×10^{-3}	
solid (77 K)	GFA	n.a.	$<2 \times 10^{-7}$	5×10^{-6}
	MCR-ALS/EFA	n.a.	2×10^{-6}	5×10^{-6}
	MCR-ALS/GFA	n.a.	2×10^{-6}	6×10^{-6}
solid (243 K)	GFA	n.a.	n.a.	only higher oligomers

[a] The concentrations presented correspond to the initial MB concentration, at which the fraction ratio of a species (or their mixtures) reaches 0.5 (data from Figures 1b−3b and 5b−7b). M = monomer; D = dimer; T = trimer. [b] GFA, the Gaussian fitting analysis; MCR-ALS/EFA, the MCR-ALS method using input data calculated by evolving factor analysis; MCR-ALS/GFA, the MCR-ALS method using input data from the Gaussian fitting analysis.

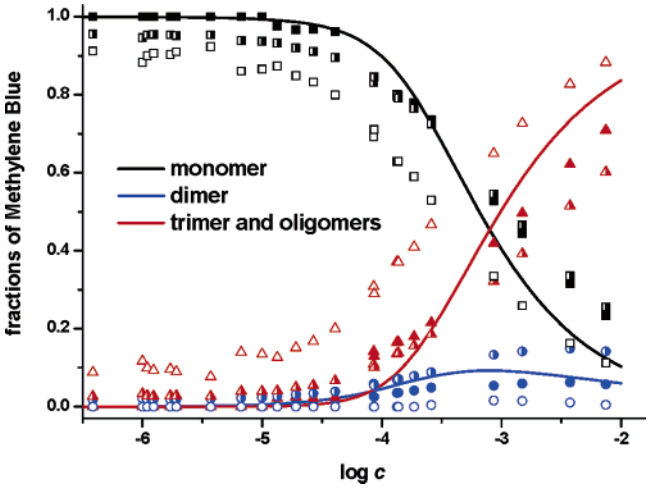

Figure 4. Comparison of all calculated concentration profiles applied for monomer (squares), dimer (circles), and trimer and oligomers (triangles). The lines represent the profiles obtained from the estimated equilibrium constants. The solid symbols were taken from the Gaussian fitting analysis (Figure 1b), the empty symbols from MCR-ALS with EFA (Figure 2b), and the half-filled ones from the MCR-ALS method using the Gaussian fitting analysis (Figure 3b).

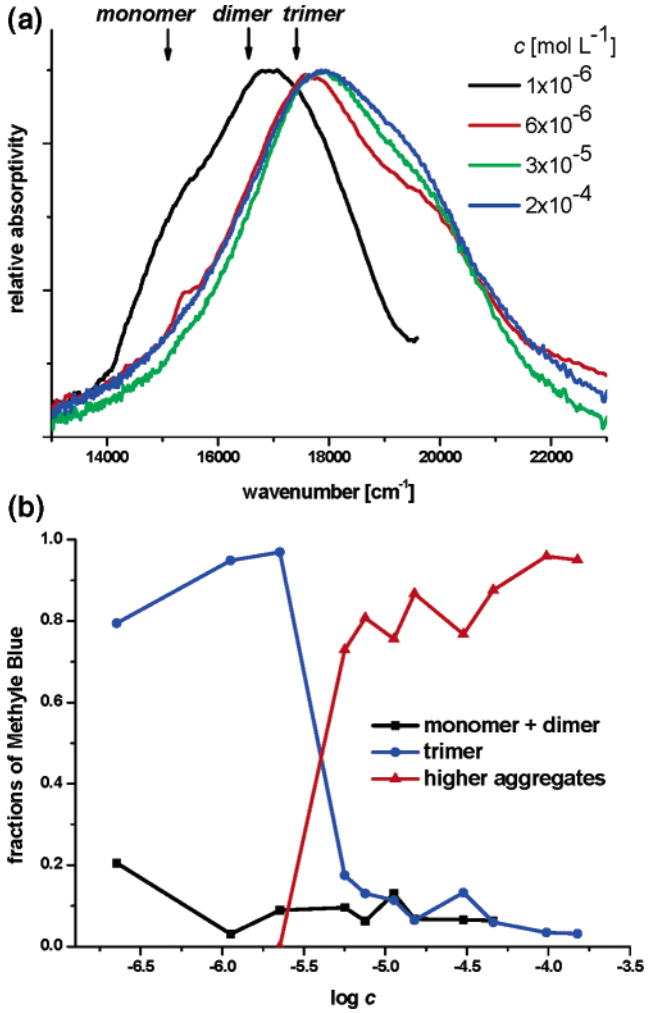

Figure 5. (a) Normalized representative spectra of MB in frozen aqueous solutions at 77 K obtained from the Gaussian fitting analysis. The arrows show the known wavenumber values[22,25] corresponding to the absorption maxima of individual species. (b) The calculated relative concentration-dependent abundance profiles in samples at 77 K as a function of the MB concentration *c* on the basis of spectra shown in Figure 5a. The lines are visualized trends of the corresponding calculated values (solid points).

4. Discussion

Both the Gaussian curve analysis and the multivariate curve resolution−alternating least squares method provided excellent tools to evaluate qualitatively as well as quantitatively the distribution of the MB species in the liquid solutions with comparable results (Figures 1−4). The first part of this study confirmed the reported findings,[22,25] according to which monomer dominates in the lowest sample concentrations (in this work $c > 5 \times 10^{-7}$ mol L^{-1}), being replaced by dimer and trimer via an effective aggregation process already detectable at $c > 10^{-4}$ mol L^{-1}. The concentration profiles calculated exclusively from the input data using EFA (Figure 2b) gave satisfactory, yet somewhat altered, results. While a lower dimer concentration is attributed to overlying (unresolved) peaks of both monomer and trimer in the calculated spectra as well as a high molar absorption coefficient of dimer (see Supplementary Information), the concentration ratios of the monomer and trimer formation profiles remained comparable in all computational methods used. Additionally, the MCR-ALS method using the Gaussian fitting analysis provided more satisfactory results, which provided data in a good agreement with those calculated using the equilibrium constants (Figure 4; Supplementary Information). Thus, all approaches described provided an authenticated and complex analysis, which advocated their use for the spectroscopy of the frozen MB solutions. Table 1 shows a summary of the quantitative analysis on the basis of the calculation methods applied. The initial concentrations of MB, at which the concentration fraction ratio of a species (or their mixtures) reaches 0.5 (50%), were deduced from in Figures 1b−3b and 5b−7b. Such values represent the possibility to compare the mathematical approaches but most importantly to evaluate the aggregation processes that occur in different media.

During the freezing process, the solutes in aqueous solutions are excluded from the growing ice phase resulting in increased concentrations on the crystal surfaces.[7,8] MB is relatively well

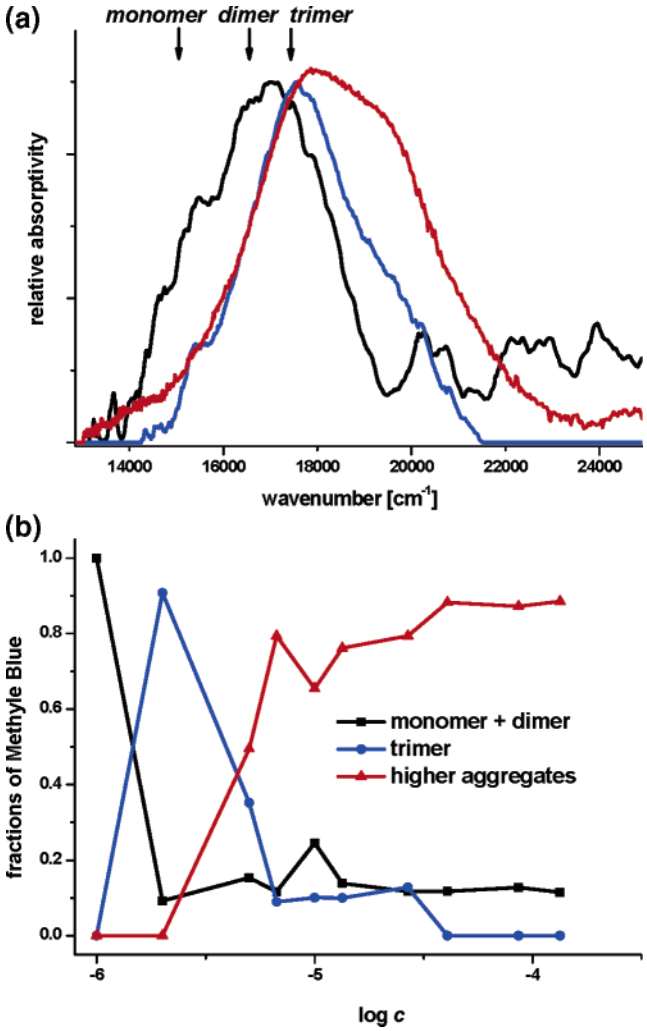

Figure 6. (a) Calculated spectra of three mathematically resolved species (generally corresponding to monomer + dimer, black; trimer, blue; trimer + higher aggregates, red) in frozen aqueous solutions at 77 K obtained from the MCR-ALS method using input data calculated by the evolving factor analysis (EFA). The arrows show the known wavenumber values[22,25] corresponding to the absorption maxima of individual species. (b) The calculated relative concentration-dependent abundance profiles in samples at 77 K as a function of the MB concentration c obtained from the MCR-ALS method on the basis of data from Figure 6a. The lines are visualized trends of the corresponding calculated values (solid points).

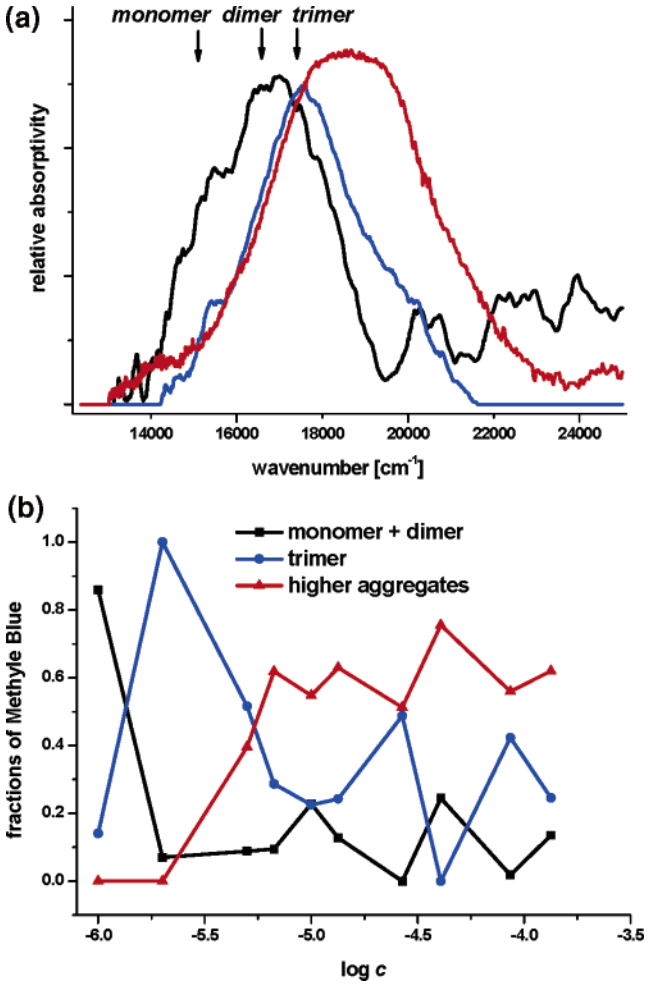

Figure 7. (a) Calculated spectra of three mathematically resolved species (generally corresponding to monomer + dimer, black; trimer, blue; trimer + higher aggregates, red) in frozen aqueous solutions at 77 K obtained from the MCR-ALS method using input data from the Gaussian fitting analysis. The arrows show the known wavenumber values[22,25] corresponding to the absorption maxima of individual species. (b) The calculated relative concentration-dependent abundance profiles in samples at 77 K as a function of the MB concentration c obtained from the MCR-ALS method on the basis of the data from Figure 7a. The lines are visualized trends of the corresponding calculated values (solid points).

soluble in water and to avoid the formation of a liquid layer in the grain boundary because of the freezing point depression, all absorption spectra were measured below 243 K when all solutions were solidified. Higher surface-layer concentration of the solutes shortens the average intermolecular distances and enhances the probability of aggregation processes. In addition, a lower temperature suppresses diffusion and molecular dynamics. Molecular aggregations in ice may change the absorption characteristics of the organic molecules because of changed interactions with the host water molecules of the cavity as well as intermolecular interactions among the solute molecules themself.[9,10] Furthermore, gaseous solutes (air) can cause the scattering of light because of fine dispersed bubbles, which in addition to reflection decrease the signal-to-noise ratio in the spectra.[36]

The relatively fast freezing rate of the aqueous MB samples immersed in a liquid nitrogen bath (77 K) caused an occurrence of new significant blue-shifted absorption bands, suggesting a change of the relative abundances of the MB species. Figures 5−7 show the results from the Gaussian curve and the MCR-ALS analyses of absorption spectra. It is apparent that self-organization of the dye occurred at the lowest bulk concentrations used; trimer dominated already at $c \sim 10^{-7}$ mol L^{-1} (Table 1), while the concentrations of both monomer and dimer were negligible. This indicates that the local concentration of MB at the grain boundaries increased by ~3 orders of magnitude upon the freezing process compared to the liquid phase. When temperature is decreased, the solute concentration at the grain boundaries becomes gradually higher until the layer solidifies. There is only a limited time to establish an equilibrated distribution of the solute molecules in quickly frozen samples at 77 K, which can be, for example, connected to an acceleration of various chemical processes because of emerged interfacial electrostatic forces.[8,37] Such forces might inhibit or enhance the repulsion of the cationic MB from grain surface layers, but we currently have no evidence for such interactions. Once the solidification is accomplished at such a low temperature, molecular diffusion is practically prevented.[38] Our recent cage effect studies on photodecarbonylation of dibenzyl ketones in frozen aqueous solutions have shown that diffusion of the benzyl

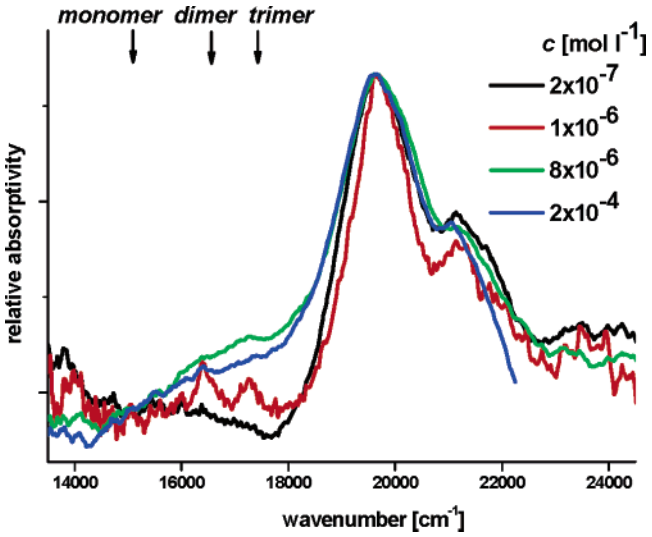

Figure 8. Normalized representative spectra of MB in frozen aqueous solutions at 243 K obtained from the Gaussian fitting analysis. The arrows show the known wavenumber values[22,25] corresponding to the absorption maxima of individual species.

radicals within aggregates at the grain boundary is still remarkably efficient at 223 K but totally restricted at 193 K, independently of the initial ketone concentration in the range of 10^{-6} to 10^{-4} mol L^{-1}.[39] Thus, MB aggregations in quickly frozen samples at 77 K must be fixed in their positions and structure. In more concentrated MB samples, the new bands at $>18\,000$ cm^{-1} most probably represent the transitions corresponding to higher aggregates as observed elsewhere.[29] All analyses concurred that such oligomers dominated at $c > 5 \times 10^{-6}$ mol L^{-1}. A minor shift due to the polarity or a different charge distribution at the phase boundary is possible, however, the MB absorption maxima are not very sensitive to the solvent polarity.[20] Since no absorption bands at lower wavenumber appeared, the formation of the head-to-tail aggregates (J-aggregates) were not expected to occur under such experimental conditions.

Higher aggregates, exhibited as two broad absorption bands between 18 000 and 22 000 cm^{-1}, were exclusively formed when the samples were frozen slowly at 243 K (Figure 8) and, furthermore, it was found that those spectra did not change upon additional cooling to 77 K. Only insignificant broad absorption in the region of 15 000−18 000 cm^{-1} advocates the existence of dimers or trimers. Such a slow freezing, requiring several minutes to complete, had to allow reaching the equilibrium before the layers solidified but it is probable that limited diffusion at subeutectic quasi-liquid layer[4] was still present during the absorption measurements. When the local concentration of the MB molecules at the grain boundaries escalates, electrostatic attraction causing the self-assembling process is more accessible, and water molecules are constrained to the ice phase. Under such conditions, the local MB concentration was raised at least by a further 3 orders of magnitude (Table 1), but most likely more, compared to the quickly frozen samples, that is more than 6 orders of magnitude compared to a liquid solution. Since we were unable to measure spectra of more diluted samples to detect the absorption band of monomer, this number is only a low estimate. Furthermore, the aggregation process was found irreversible in the temperature range 243−77 K once solidification occurred; thus, the intermolecular binding prevented the diffusion and the process was fully equilibrated. The fact that the absorption spectra were practically independent of the initial MB concentration suggests that the composition of aggregates in the quasi-liquid layer (243 K) was identical. On the basis of the solute molality (m_s) calculation from the cryoscopic constant K_f ($\Delta T = K_f m_s$, where ΔT is the freezing point depression and $K_f = 1.858$ K mol^{-1} kg for H_2O), we can estimate that the MB concentration at 243 is about 10 mol kg^{-1} if the layer is still liquid. Such a value corresponds to 5−8 orders of magnitude increase in the local concentration, depending on the initial concentration, and it is in accord with our estimate on the basis of the absorption study. This is fairly consistent with previous observations from Takenaka et al.[8] and us[9], in which an increase in the local concentration of various solutes over such a magnitude was calculated from the freezing point depression measurements. Furthermore, Cho and collaborators showed that subeutectic quasi-liquid (quasi-brine) phase can coexist with ice and solid $NaCl{\cdot}2H_2O$ at temperatures as low as 228 K[4] when the state of equilibrium is achieved, suggesting that there are many similarities in the behavior of inorganic and organic contaminants in ice.

The concentration-enhancing effect in the partially frozen aqueous solutions has been described since the 1960s in connection with the acceleration of some reactions.[7,8,40−43] Such knowledge is extremely valuable also for the photochemical studies in ice or snow since most of the reactions already observed so far were bimolecular.[10,15] On the basis of the above results, we present a quantitative as well as qualitative description of the aggregation process in the frozen aqueous solutions that may represent a general behavior of small organic molecules as ice contaminants. Further absorption and emission experiments, especially with realistic contaminant concentrations, will be required to explore in order to understand more the physical and chemical processes in terrestrial and atmospheric ices.

Acknowledgment. The project was supported by the Czech Ministry of Education, Youth and Sport (MSM 0021622412) and by the Grant Agency of the Czech Republic (205/05/0819). The authors express their thanks to P. Dvorak, J. Klanova, A. Rokosova, and J. Topinkova for valuable discussions. We are grateful to anonymous reviewers who have contributed substantially by some constructive critical comments. This paper contributes to the Air-Ice Chemical Interactions (AICI) task of IGAC and SOLAS.

Supporting Information Available: The descriptions of the Gaussian curve fitting and equilibrium constants calculations are included in the supporting material. This material is available free of charge via the Internet at http://pubs.acs.org.

References and Notes

(1) Wang, S. Y. *Nature* **1961**, *190*, 690.
(2) Petrenko, V. F.; Whitworth, R. W. *Physics of ice*; Oxford University Press: Oxford, U.K., 1999.
(3) Dash, J. G.; Fu, H. Y.; Wettlaufer, J. S. *Rep. Prog. Phys.* **1995**, *58*, 115.
(4) Cho, H.; Shepson, P. B.; Barrie, L. A.; Cowin, J. P.; Zaveri, R. *J. Phys. Chem. B* **2002**, *106*, 11226.
(5) Doppenschmidt, A.; Butt, H. J. *Langmuir* **2000**, *16*, 6709.
(6) Finnegan, W. G.; Pitter, R. L.; Hinsvark, B. A. *J. Colloid Interface Sci.* **2001**, *242*, 373.
(7) Takenaka, N.; Ueda, A.; Maeda, Y. *Nature* **1992**, *358*, 736.
(8) Takenaka, N.; Ueda, A.; Daimon, T.; Bandow, H.; Dohmaru, T.; Maeda, Y. *J. Phys. Chem.* **1996**, *100*, 13874.
(9) Klanova, J.; Klan, P.; Heger, D.; Holoubek, I. *Photochem. Photobiol. Sci.* **2003**, *2*, 1023.
(10) Klanova, J.; Klan, P.; Nosek, J.; Holoubek, I. *Environ. Sci. Technol.* **2003**, *37*, 1568.
(11) Dubowski, Y.; Hoffmann, M. R. *Geophys. Res. Lett.* **2000**, *27*, 3321.
(12) Hoffmann, M. R. Possible chemical transformations in snow and ice induced by solar (UV photons) and cosmic irradiation (muons). In *NATO ASI Series I*, 1996; Wolff, W., Bales, R. C., Eds.; Vol. 43, p 353−377.

(13) Klan, P.; Holoubek, I. *Chemosphere* **2002**, *46*, 1201.
(14) Blaha, L.; Klanova, J.; Klan, P.; Janosek, J.; Skarek, M.; Ruzicka, R. *Environ. Sci. Technol.* **2004**, *38*, 2873.
(15) Klan, P.; Klanova, J.; Holoubek, I.; Cupr, P. *Geophys. Res. Lett.* **2003**, *30*, art. no. 1313.
(16) Domine, F.; Shepson, P. B. *Science* **2002**, *297*, 1506.
(17) Masclet, P.; Hoyau, V.; Jaffrezo, J.; Legrand, M. *Analusis* **1995**, *23*, 250.
(18) Toom-Sauntry, D.; Barrie, L. A. *Atmos. Environ.* **2002**, *36*, 2683.
(19) Wania, F. *Environ. Sci. Pollut. Res.* **1999**, *6*, 11.
(20) Parkanyi, C.; Boniface, C.; Aaron, J. J.; Maafi, M. *Spectrochim. Acta, Part A* **1993**, *49*, 1715.
(21) Lewis, G. N.; Goldschmid, O.; Magel, T. T.; Bigeleisen, J. *J. Am. Chem. Soc.* **1943**, *65*, 1150.
(22) Bergmann, K.; O'Konski, C. T. *J. Chem. Phys.* **1963**, *67*, 6169.
(23) Cenens, J.; Schoonheydt, R. A. *Clays Clay Miner.* **1988**, *36*, 214.
(24) Kemnitz, K.; Tamai, N.; Yamazaki, I.; Nakashima, N.; Yoshihara, K. *J. Phys. Chem.* **1986**, *90*, 5094.
(25) Braswell, E. *J. Chem. Phys.* **1968**, *72*, 2477.
(26) Lee, C.; Sung, Y. W.; Park, J. W. *J. Phys. Chem. B* **1999**, *103*, 893.
(27) Ruprecht, J.; Baumgartel, H. *Ber. Bunsen-Ges. Phys. Chem. Chem. Phys.* **1984**, *88*, 145.
(28) Zhao, Z. M.; Malinowski, E. R. *J. Chemom.* **1999**, *13*, 83.
(29) Jockusch, S.; Turro, N. J.; Tomalia, D. A. *Macromolecules* **1995**, *28*, 7416.
(30) Gessner, F.; Schmitt, C. C.; Neumann, M. G. *Langmuir* **1994**, *10*, 3749.
(31) Jaumot, J.; Avino, A.; Eritja, R.; Tauler, R.; Gargallo, R. *J. Biomol. Struct. Dyn.* **2003**, *21*, 267.
(32) Multivariate Curve Resolution Homepage. http://www.ub.es/gesq/mcr/mcr.htm (accessed Jan 2005).
(33) Tauler, R.; Izquierdoridorsa, A.; Casassas, E. *Chemom. Intell. Lab. Syst.* **1993**, *18*, 293.
(34) Petrov, V.; Antonov, L.; Ehara, H.; Harada, N. *Comput. Chem.* **2000**, *24*, 561.
(35) Antonov, L. *TrAC, Trends Anal. Chem.* **1997**, *16*, 536.
(36) Mesquita, O. N.; Ladeira, L. O.; Gontijo, I.; Oliveira, A. G.; Barbosa, G. A. *Phys. Rev. B* **1988**, *38*, 1550.
(37) Takenaka, N.; Furuya, S.; Sato, K.; Bandow, H.; Maeda, Y.; Furukawa, Y. *Int. J. Chem. Kinet.* **2003**, *35*, 198.
(38) Gudipati, M. S. *J. Phys. Chem. A* **2004**, *108*, 4412.
(39) Ruzicka, R.; Barakova, L.; Klan, P. *J. Phys. Chem. B* **2005**, *109*, 9346.
(40) Grant, N. H.; Clark, D. E.; Alburn, H. E. *J. Am. Chem. Soc.* **1961**, *83*, 4476.
(41) Bruice, T. C.; Butler, A. R. *J. Am. Chem. Soc.* **1964**, *86*, 4104.
(42) Butler, A. R.; Bruice, T. C. *J. Am. Chem. Soc.* **1964**, *86*, 313.
(43) Fennema, O. Reaction Kinetics in Partially Frozen Aqueous Systems. In *Water relations of foods*; Duckworth, R. G., Ed.; Academic Press: London, 1975; p 539.